ADVANCED QUANTUM TECHNOLOGIES
www.advquantumtech.com

Magnetic Molecules as Building Blocks for Quantum Technologies

*Eufemio Moreno-Pineda and Wolfgang Wernsdorfer**

Since the initial observation of quantum effects, scientists have worked diligently to understand and harness their potential. Thanks to many pioneers, a level where quantum effects can be exploited is reached. Numerous cutting-edge technologies, such as quantum sensing and quantum computing, are proposed. A common trait in all technologies is the need to manipulate and read out their states; therefore, the quantum characteristics of the building blocks must adhere to strict guidelines. Magnetic Molecules (MMs) are promising candidates. They can be obtained indistinguishably, and the control over their structural and electronic properties, makes them appealing to act as quantum bits or "qubits". MMs can be connected to other units while preserving their coherence properties, enabling the implementation of quantum gates. Furthermore, the low-lying energy levels can be exploited as qudits, which can exist in more than 2 states simultaneously ($d > 2$), allowing them to hold more information efficiently. The larger electronic/nuclear space in qudits can decrease the number of physical units and enhance computational efficiency, reducing error and making them promise for complex problem-solving. In this perspective article, the physical characteristics of MMs and key achievements that position them as promising candidates for quantum technologies, are described.

1. Introduction

Numerous benefits are anticipated for the exploitation of quantum phenomena in real-world applications. For instance, by utilizing quantum coherence and entanglement, it would be possible to observe minuscule fluctuations, not achievable by classical sensing devices, providing new sensing capabilities with applications spanning from physics to biology.[1–9] Furthermore, as suggested by Feynman[10] and Lloyd,[11,12] quantum effects could also enable the simulation of classically untreatable quantum mechanical problems, thus, creating a quantum computer is one of the most appealing goals. A quantum computer would make it possible to complete tasks currently impossible or exceedingly difficult, such as factoring large numbers, fast computation of sizeable problems, and simulating quantum mechanical problems truly universally, among others. The fact that the current manufacturing technologies approach the quantum size limit, further acts as a driving force for understanding and integrating quantum effects in novel technologies. Expectedly, the foreseen potential of a quantum computer prompted intensive investigation of several consortiums.[13–16]

Implementing quantum technologies, however, requires scaffolds fulfilling certain characteristics. Although several systems are actively studied as the basic unit of quantum computers, that is, the quantum bit or "qubit", MMs could be superior qubits compared to other common platforms. This is due to their inherent advantages in scalability and tunability,[17–20] which makes possible their integration into devices. MMs benefit from the bottom-up synthetic approach, allowing for the creation of large arrays of identical qubits, which is crucial for scaling up quantum systems.[17–20] This aspect is considered a major challenge for common platforms such as spin impurities[21] or semiconductor quantum dots.[22] Moreover, through a sensible design, the physical properties of these systems – environmental, electronic, and nuclear properties – can be engineered to a large extent, allowing the enhancement of their coherence characteristics, and direct interunit coupling, a prerequisite for the realization of quantum gates. The so-generated quantum states, electronic and nuclear, can be subsequently controlled using external fields, offering versatile tunability.

Additionally, several studies have demonstrated that the precise control over the chemical and physical characteristics of

E. Moreno-Pineda
Facultad de Ciencias Naturales, Exactas y Tecnología
Departamento de Química-Física
Universidad de Panamá
Panamá 0824, Panamá

E. Moreno-Pineda
Facultad de Ciencias Naturales
Exactas y Tecnología, Grupo de Investigación de Materiales
Universidad de Panamá
Panamá 0824, Panamá

E. Moreno-Pineda, W. Wernsdorfer
Physikalisches Institut
Karlsruhe Institute of Technology
D-76131 Karlsruhe, Germany
E-mail: Wolfgang.Wernsdorfer@neel.cnrs.fr,
wolfgang.wernsdorfer@kit.edu

W. Wernsdorfer
Institute for Quantum Materials and Technology (IQMT)
Karlsruhe Institute of Technology (KIT)
Hermann-von-Helmholtz-Platz 1, D-76344 Eggenstein-Leopoldshafen, Germany

The ORCID identification number(s) for the author(s) of this article can be found under https://doi.org/10.1002/qute.202300367

DOI: 10.1002/qute.202300367

MMs allows for tailoring their electronic and hyperfine properties, making them suitable qu*d*its (where $d > 2$)[18,19,23] candidates. Unlike the two-level qubits units, qu*d*its can be designed with accessible low-lying electronic and nuclear levels, serving as ancillary states for quantum computations within a single entity. This enables the execution of quantum algorithms without needing interconnection with another qubit/qu*d*it unit. Qu*d*its offer several advantages over qubits in quantum computing: their higher-dimensional state space allows for denser information encoding and enhanced parallelism by enabling simultaneous manipulation of multiple states, thus accelerating certain quantum algorithms. Moreover, implementing quantum gates with qu*d*its can be simpler, requiring fewer gates for equivalent computational power. Importantly, the multilevel nature of qu*d*its can be used to protect information against errors, addressing a significant challenge in all qubit platforms.[24–28] In this perspective article, we review some important characteristics of MMs that would allow the integration of these systems into cutting-edge technological applications. Herein, we highlight some important results in the field of MMs and the advantages of these systems as part of novel technologies. The goal of this perspective article is twofold: *i*) to highlight the advantages of molecular systems and the chemical control over their key physical aspects through chemical design; *ii*) to attract more experimentally as well as theoreticians working with nonmolecular quantum systems, to dive into the field, to test more of the myriads of molecular systems chemists can produce.

2. Magnetic Molecules and Quantum Effects

Quantum technologies rely on observed quantum effects. MMs have shown bewildering quantum properties, particularly those exhibited by molecules possessing an energy barrier to the relaxation of the magnetization, the so-called Single Molecule Magnets (SMMs). The properties exhibited by SMMs have led to their integration into hybrid devices, emphasizing their quantum nature. By leveraging this approach, spintronic molecular devices enabled the manipulation and reading of spin states, facilitating the implementation of quantum algorithms. In the subsequent section, we briefly show some key characteristics of MMs relevant to quantum technology proposals. Note that in this work, we refer to MMs as any magnetic molecule, while the SMM term is exclusively used for MMs, which shows a barrier to the relaxation of the magnetization.

2.1. Well-Defined Anisotropic Ground State

The observation of large anisotropy of the ground states in MMs was first evidenced in a $[Mn_{12}(\mu_3\text{-}O_{12})(CH_3COO)_{16}(H_2O)_4]\cdot 2CH_3COOH\cdot 2H_2O$ (or Mn_{12}) complex[29] (**Figure 1A**). The ground state of the Mn_{12} is an $S_T = 10$, arising from the strong interaction between the Mn^{3+} and Mn^{3+} ions composing the system and the small, yet important, Spin-Orbit Coupling (SOC). The anisotropy of the Mn_{12} is described by the spin Hamiltonian: $\mathcal{H} = DS_z^2 + E(S_x^2 + S_y^2)$, where D is the zero-field splitting parameter, and E is the rhombic term. The effect of D is to quantize the S state leading to the $m_S = -S...S$ being doubly degenerated. Consequently, the energy of the system follows a parabolic behavior with an energy barrier $U_{eff} = -|D|S_T^2$ (Figure 1B). Each side of the parabola corresponds to an opposed orientation of the magnetic moment; hence D provides an estimate of the barrier reorientation of the magnetic moment. Further studies show that the spin of the Mn_{12} complex remains frozen below the blocking temperature (T_B) of ca. 4 K.[30] Due to the ability of this system to retain magnetization below T_B, systems possessing such characteristics were coined single-molecule magnets. Technologically, a barrier to the reorientation of the magnetization implied the possibility of storing information at the molecular level, thus, arising proposals to integrate MMs into technologies. Due to the spin dependence of the energy barrier, polymetallic systems were sought during the first decade of investigation. However, despite the efforts and many investigated polymetallic complexes, the Mn_{12} remained the SMM with the highest anisotropy, with the largest observed hysteresis at low temperatures ($T_B \approx 4$ K).

Remarkably, in 1996, scientists made an impressive discovery: single crystals of Mn_{12} exhibit Quantum Tunnelling of Magnetisation (QTM) (Figure 1C), a highly sought-after mesoscopic phenomenon.[31] QTM allows the reversal of the electronic state through the barrier, due to the mixing of the quantum states on opposite sides of the barrier. This finding marked an important milestone in the study of quantum phenomena.

A new era for molecular magnetism began in 2003 when Ishikawa first observed an energy barrier to the relaxation in single lanthanide ion complexes with the formula TBA[$LnPc_2$] (where Ln = Tb^{3+} and Dy^{3+})[32] (Figure 1D). The barrier for the Tb^{3+} analog was an order of magnitude larger than the one for Mn_{12}. The origin of the anisotropy is the strong intrinsic SOC in lanthanides, resulting in a highly anisotropic ground state with a significant magnetic moment. Consequently, there was no necessity for polymetallic systems to achieve large magnetic states. For $[TbPc_2]^-$ a $J = 6$ ($S = 3$ and $L = 3$) characterizes its magnetic state, with a large separation between the $J = 6$ and $J = 5$ levels of ca. 2900 K. The large separation between the J states ensures that only the $J = 6$ multiplet is populated at normal conditions. In the molecular structure, the Tb^{3+} ion possesses a D_{4h} symmetry, which can be described in Stevens formalism by a ligand field spin Hamiltonian of the form:[33]

$$\mathcal{H}_{lf} = \sum_{n=1}^{3} B_{2n}^0 O_{2n}^0 + B_4^4 O_4^4 + B_6^4 O_6^4 \quad (1)$$

where B_q^k are experimentally determined parameters. The ligand field lifts the degeneracy of the $2J+1$ states of the $J = 6$ multiplet, rendering a $m_J = \pm 6$ ground state with a separation of ca. 600 K from the $m_J = \pm 5$ first excited states (Figure 1E). Experimentally, it has been found that the ligand field acting upon the Tb^{3+} ion generates a quantization axis for the $m_J = \pm 6$ ground state perpendicular to the Pc plane.

Another remarkable characteristic of $[TbPc_2]^-$, and in general in lanthanide-based systems, is their strong hyperfine coupling, which causes the electronic spin to couple strongly to the nuclear spin, $I = 3/2$ for Tb^{3+}. The spin Hamiltonian of hence takes the form:[34,35]

$$\mathcal{H}_{TbPc_2} = \mathcal{H}_{lf} + \mu_B \mu_0 H \hat{g} J + A_{hyp} I \cdot J + I \hat{P}_{quad} I \quad (2)$$

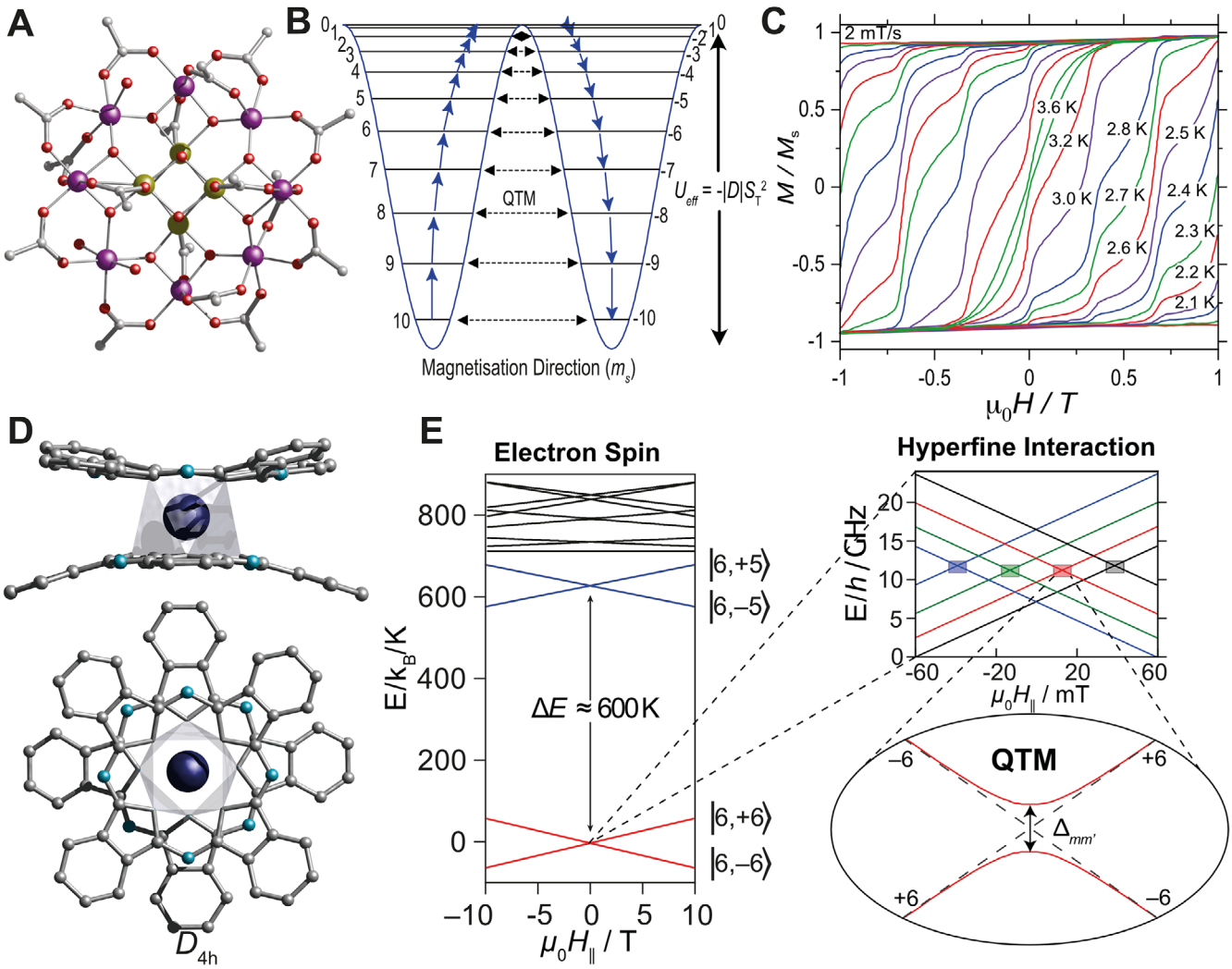

Figure 1. Anisotropy and QTM molecular magnets. A) Molecular structure of Mn_{12} complex; B) Schematic representation of quantization of the electronic energy level of Mn_{12} with $S_T = 10$. The reversal of the magnetization follows through the m_S states (blue arrows) via phonon absorption (excitation of the spin system to the top of the barrier) and emission (de-excitation to the bottom of the other side of the barrier); C) Temperature-dependent hysteresis loops for Mn_{12} revealing QTM steps; D) Molecular structure of $[TbPc_2]^{\pm/0}$ (top) side and (bottom) top view. The polyhedral highlights the TbN_8 coordination environment with D_{4h}-square-antiprismatic coordination geometry. E) (left) Electronic energy level for TBA[$TbPc_2$]. (Right) The zoomed region shows the hyperfine split (by $I = 3/2$) ground doublet with $m_I = -3/2$ (black), $-1/2$ (red), $+1/2$ (green) and $+3/2$ (blues) square regions. The zoomed region of the hyperfine levels shows the avoided level crossing arising from transverse fields, where reversal can occur *via hf*-QTM. Color code in panels (A) and (D): Mn^{3+}, violet; Mn^{4+}, dark yellow; Tb, dark blue; C, grey; N, cyan; O, red. Hydrogens were omitted for clarity. Figure C) adapted from ref. [30] Copyright 2006, American Chemical Society. Figure (E) adapted from ref. [19] with permission from the Royal Society of Chemistry.

the second term is the Zeeman interaction, and the third and fourth terms are the hyperfine and quadrupolar interaction, respectively. The hyperfine interaction splits the $m_J = 6$ state into $2I+1$ levels, i.e., $m_I = +3/2$, $+1/2$, $-1/2$, and $-3/2$, while the quadrupolar term couples the electric field gradient of the magnetic moment, causing an uneven separation between m_I states (zoomed region inC Figure 1E (right)); this playing an important role for the manipulation of the hyperfine levels and the realization of the Quantum Grover's algorithm.[36] Thanks to a thorough understanding of the magnetic characteristics of SMMs, it has been possible to realize the design criteria[37–39] leading to the remarkably high barriers,[40–44] open hysteresis up to 80 K[44] and large coercive fields[43,45] These characteristics make SMMs excellent candidates for data storage devices.

2.2. Relaxation Characteristics

Ideally, the electronic ground state in SMMs is expected to remain frozen below a threshold temperature, while above it, temperature-dependent relaxation mechanisms become dominant. In practice, however, the systems relax via several thermally activated processes, active well below the threshold temperature. Phonon-assisted mechanisms contribute to the relaxation of the

magnetization by modifying the ligand field via vibrations. These vibrations create a modulation on the crystal field, promoting transitions between the different spin states via optical and acoustic phonons. Depending on the type of ion involved—Kramers or non-Kramers ions—these processes can entail the absorption and emission of one or 2 phonons. In Kramers ions the degeneracy can be fully removed, whereas in non-Kramers ions, a minimum degeneracy of 2 always remains. Overall, the relaxation dynamics of magnetic molecules are primarily influenced by three processes: *i*) the Orbach process, the Raman process *ii*), and *iii*) the direct process. In the direct process, one energy phonon is released because of relaxation. In the Orbach and Raman, phonons are absorbed and reemitted as part of the relaxation process. In the Orbach process relaxation proceeds via a real state, whereas in the Raman mechanism, it relaxes by entering a virtual excited state. Obtaining a comprehensive grasp of these processes is crucial for effectively employing magnetic molecules in roles such as spin qubits and memory devices. Great advances in this direction have been put forward experimentally and theoretically,[46–52,54] hence providing the recipes for the chemical design of robust molecular qubits with long coherence times.[42–44,55] As a rule of thumb, relaxation can be decreased by engineering the correct ligand field in which the lanthanide is embedded, i.e., axial or equatorial, contingent upon the lanthanide ion, increasing the rigidity of the coordinating ligands, thus creating high energy intramolecular vibration (optical phonons) and by intermolecular separation of the magnetic units by bulky ligands (acoustic phonons).

An additional relaxation pathway, significant for the vast majority of SMMs, is QTM. Most SMMs, lose their magnetisation even at sub-Kelvin at temperatures through this non-thermally activated mechanism.[56] QTM permits spin reversal below the energy barrier due to a superposition of the $\pm m_J$ states. The degeneracy at the crossing is hence converted into an avoided level crossing, with a separation $\Delta_{m,m'}$. The avoided crossing is related to the transverse anisotropy terms and transverse magnetic fields. At the crossing the eigenvectors of the Hamiltonian are a linear combination of the positive and negative spin projection, hence at this point, there is a finite probability of the spin to be at both sides of the barrier, causing the spins to tunnel between the states. The tunneling probability between states, upon sweeping the field through the crossing, is given by the Landau-Zener-Stückelberg (LZS) model:

$$P_{LS} = 1 - exp\left(-\pi\omega_T \frac{\delta H_0}{\alpha}\right) \quad (3)$$

where ω_T is the angular frequency of oscillation between states m and m', which is related to the tunnel splitting by $\Delta_{m,m'} = 2\hbar\omega_T^{m,m'}$. The field interval where tunneling is predicted to occur is given by $\delta H_0 = \frac{\Delta_{m,m'}}{g\mu_B\mu_0|m-m'|}$, known as bare tunnel width.

Hyperfine-driven QTM (*hf*-QTM) has been observed in $[LnPc_2]^-$ (where Ln = Tb^{3+}, $^{163}Dy^{3+}$, and Ho^{3+}) in μSQUID studies.[34,35,57] In general, despite the large separation between the ground and the first excited state in $[TbPc_2]$, QTM is expected to be active at the zero-field crossing (Figure 1E). However, thanks to the strong hyperfine interaction, this crossing is split into 4 (zoomed region in Figure 1E), leading to *hf*-QTM, acting as relaxation pathways for the magnetization.[34] This effect has been observed in several MMs. Notice that although QTM acts as temperature-independent relaxation pathways, considered a nuisance for high-density data storage applications, it plays an important role in the initialization, manipulation, and read-out of nuclear spins in the $TbPc_2$ complex.[36] QTM has also allowed the read-out of the hyperfine-coupled nuclear spin states of a Tb_2Pc_3 SMM in a single crystal[58] and a spin transistor configuration.[59]

2.3. Coherence

MMs have been shown to possess long coherence times, an important aspect of their implementation in quantum technologies. Long coherence times allow the realization of logical operations without losing the information before the operation has been completed. The coherence is evaluated by 2 parameters: the spin-lattice relaxation time, T_1 and the spin-spin relaxation time T_2. While T_1 describes the time taken for the magnetization to return to the thermal equilibrium (along the *z*-axis) after being tipped 90°, T_2 is the time taken by the magnetization to decay on the *xy*-plane after being tipped 90° from the z-axis – dictating the superposition lifetime required for computation. Both relaxations are interwoven, as the coherence time is limited by T_1, as $2T_1 \geq T_2$, especially at high temperatures. The long coherence times exhibited by magnetic molecules make them plausible qubit candidates.

Advances in understanding the relaxation mechanisms in MMs have inspired the development of synthetic strategies to engineer molecules with prolonged coherence times. Experimentally, pulsed EPR has been employed to observe long coherence durations in the well-known $\{Cr_7Ni\}$ wheels.[60] The coherence periods of these systems were improved by chemical design. Furthermore, these units have been shown to continue to function reliably whether connected to one, two, or more units[61–64] which led to their suggestion for logic gates. Furthermore, a deliberate design of these systems has facilitated the mitigation of decoherence originating from their environment, resulting in improved coherence and enabling effective detection of lengthy T_1 and T_2 times at room temperature and in bulk crystals.[65,66] Long coherences in complexes based on vanadyl complexes[66–73] have also been observed, resulting in times equivalent to NV centers.[74]

An alternative approach to achieving longer coherence times involves designing magnetic systems that are intrinsically robust against noise, eliminating the need for magnetic dilution. The interaction that mixes the qubit states, such as the hyperfine interaction and/or magnetic and electric dipole moments, results in an avoided level crossing known as "clock transitions" (CT), which allows magnetic noise-tolerant systems to be created.[75–77] The outcome is long a T_2 and the spin qubits become insensitive to variations in external magnetic fields. The magnetic noise resistance of a $[Ho(W_5O_{18})_2]^{-9}$ system (HoW_{10}) with D_{4d} pseudo-axial symmetry was demonstrated leading to a long T_2 and strong resilience to magnetic field variations. Despite the magnetic field resilience and relatively long T_2, a problem with HoW_{10} was the relatively short T_1, which limits T_2. A strategy to enhance T_1 and, therefore, T_2 consists of increasing the s-orbital character, hence increasing the electron-nuclear Fermi constant and decreasing the SOC.[78] This strategy has been exemplified in a Lu^{+2} MM,

yielding T_1 of the ms order and T_2 exceeding 10 µs. These results highlight how rational design can lead to the creation of MMs with the desired physical characteristics.

3. Single Molecule Devices

The integration of MMs in single-molecule devices has been shown to render extraordinary results, highlighting the quantum nature of the complexes and the possibility of not solely observing these effects, but also, manipulating them. By adopting this strategy, researchers have successfully developed spintronic molecular devices. These devices allow for precise control and readout of spin states, facilitating quantum operations. In the subsequent section, we present essential discoveries concerning single-molecule devices and their unique characteristics.

3.1. Single-Molecule Spin Transistors and Valves

A spin transistor refers to a three-terminal spin arrangement in which electrons can be transported across the molecule, with the molecule bridging the gap of the junction, from source to drain. Examples of magnetic molecule-transistor devices, without compromising their structural integrity,[79] are Fe_4[80] and $TbPc_2$.[36,81–85] When a single molecule of $TbPc_2$ complex is trapped in gold junctions using the electro-migration technique (**Figure 2A**), the Tb^{+3} very stable redox state and the delocalization of the π-radical over the Pc ligands allow the electron conduction while maintaining the molecule intact.[36,81–85] The π-radical and Tb^{3+} spins interact strongly, resulting in the read-out dot, which enables the measurement of conductance changes. The spin cascade reflects the transport properties of the $TbPc_2$ molecule $|S = 1/2\rangle||J = 6\rangle||I = 3/2\rangle$ (Figure 2B) thanks to the antiferromagnetic coupling between the $S = 1/2$ of the π-radical and the magnetic moment carried by the Tb^{3+} ion, as well as its hyperfine coupling to the nuclear spin states of the Tb^{3+} ion. Four sharp jumps are observed in the differential conductance after sweeping the field (Figure 2C). The jumps are caused by the *hf*-QTM, at which the electron spin of Tb^{3+} is reversed.

Detecting the spin reversals at these 4 level crossings, results in a change in the transport characteristics of the read-out dot.[81,84] Extensive investigation of this system resulted in long T_1 and T_2 of 20 and 300 µs, respectively, which allowed the execution of Grover's algorithm utilizing the 4 nuclear spin states[36] (vide infra) and realization of an iSWAP gate.[85]

To encode a larger number of hyperfine states into a single molecular unit, an extension of the archetypal $[TbPc_2]^{0/-}$ was synthesized. The system comprised two Tb^{3+} ions sandwiched between three Pc moieties, producing a triple-decker unit (Tb_2Pc_3). The anisotropy of the system is of the same order as the $[TbPc_2]^{0/-}$, with the first excited state lying at ca. 400 K (**Figure 3B**) Single crystal µSQUID studies revealed that the interaction of the electronic spin of the Tb^{3+} ions can indirectly couple the nuclear spin of the ions, due to a ferromagnetic interaction between the Tb^{3+}. As a result, the number of accessible nuclear spins is increased to sixteen ($d = 16$), as evidenced by the *hf*-driven QTM events (**Figure 3C**). Integration of an analogous Tb_2Pc_3 unit into a three-terminal transistor configuration shows that the electronic states of the system can be read out.[59] Seven nondegenerate transitions are detected in the field sweep, however, due to the uneven separation between the states, more than 7 might be available for computation, opening the door to more complex algorithms such as Fredkin and Toffoli. Importantly, contrary to the $[TbPc_2]^{0/-}$ unit, the spin lifetimes of the Tb_2Pc_3 system are found to be short, highlighting current flow through the system, hence further optimization is required (**Figure 3**).

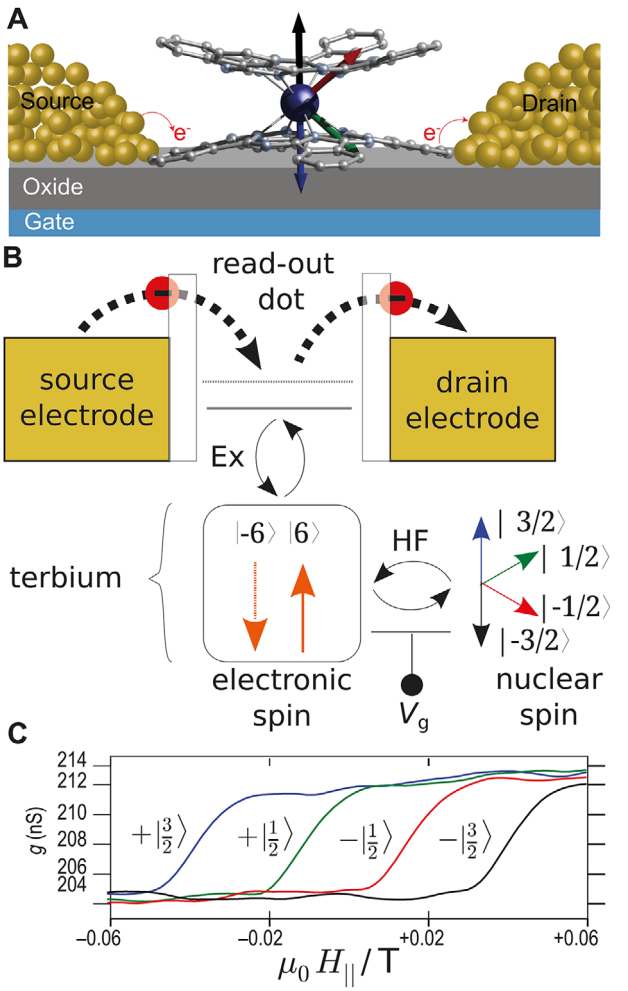

Figure 2. $TbPc_2$ Spin Transistors. A) Pictorial representation of molecular spin transistor, with a $TbPc_2$ molecule embedded between the source and drain (top) and differential conductance studies (d*I*/d*V*) as a function of drain-source voltage (V_{ds}) and gate voltage (V_g) for a $TbPc_2$ spin transistor device (bottom); B) Schematic view of the read-out cascade occurring in [$TbPc_2$] in the transistor device; C) The conductance jumps correspond to the 4 level-crossings associated with the nuclear spin $I = 3/2$ of Tb^{3+}. Panel (A) is adapted from ref. [86] Copyright 2021, Springer Nature Limited. Panels (B) and (C) from ref. [84] Copyright 2014, The American Association for the Advancement of Science.

Magnetic molecules can also be integrated into hybrid devices through a supramolecular spin valve configuration. A system with $TbPc_2$ serving as a spin dot and a carbon nanotube (CNT) acting as a read-out dot was explored by Urdampilleta et al.[87–89] allowing the determination of the electronic and nuclear spin characteristics of the Tb^{+3} ion.[87–91] Due to the robust interaction between the $TbPc_2$ molecules mounted on CNTs, read-out was possible via magneto-transport measure-

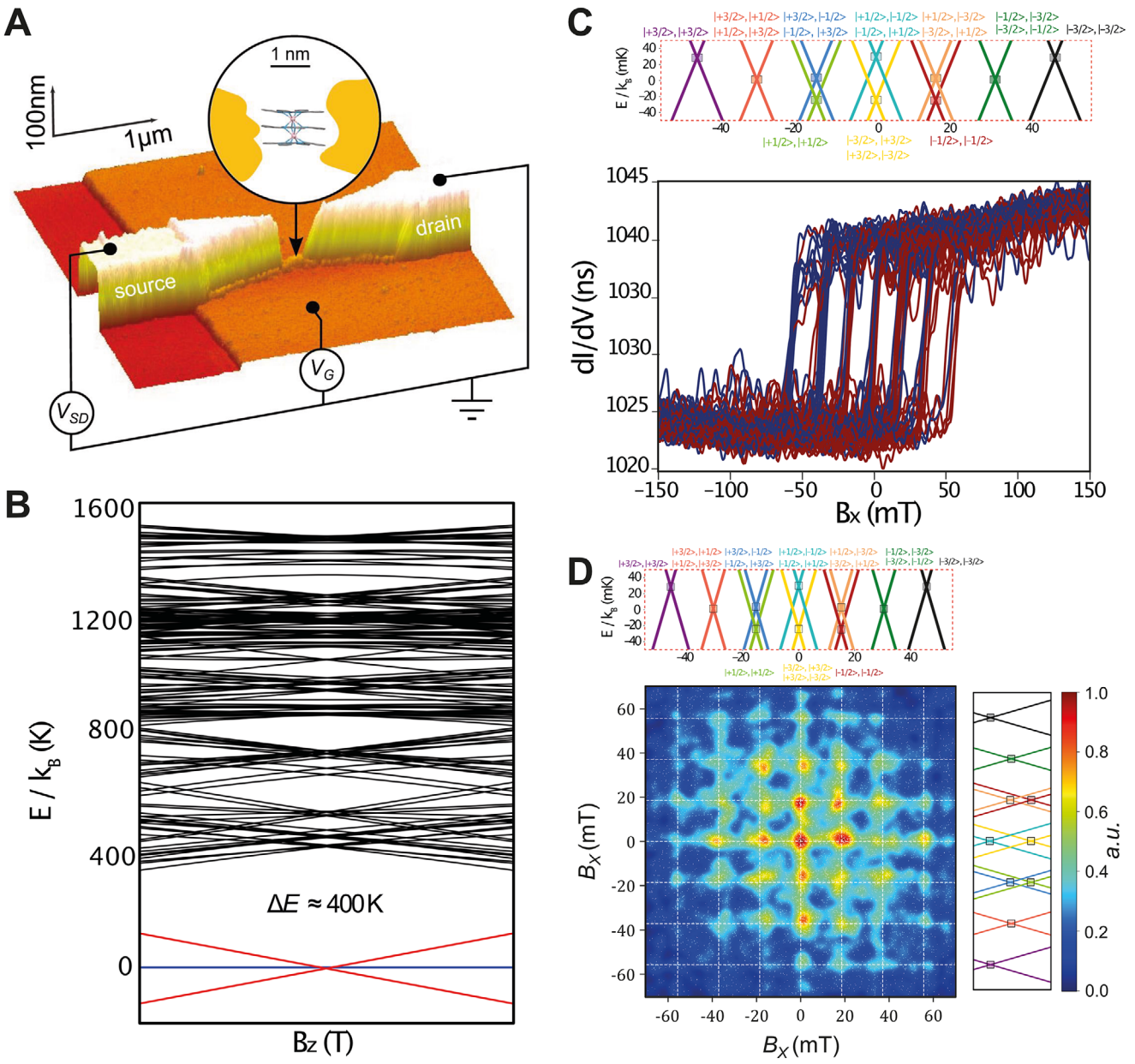

Figure 3. Quantum Spin Transistors Tb_2Pc_3. A) AFM colored image of Tb_2Pc_3 SMM connected to a gold source and drain electrodes through tunneling barriers, on top of Au/HfO_2 gate. The experimental setup allows us to control the gate potential V_G and the source-drain potential V_{SD}, while performing lock-in measurements through the latter; B) Zeeman diagram of Tb_2Pc_3 SMM with the applied magnetic field $B_{||}$ Along the easy axis of the magnetization with the separation of $\Delta E \approx 400$ K from the first excited state. C) dI/dV as a function of V_{ds} and V_g for a Tb_2Pc_3 spin transistor device. The conductance jumps correspond to spin reversal at the allowed QTM crossings. D) Spins reversals correlation measurement. The *x*-axis corresponds to conductance jumps during a magnetic field sweep, and the *y*-axis represents the conductance jumps during subsequent sweeps. Adapted from ref. [59] CC-BY 4.0 International License, Springer Nature Copyright 2021.

ments. When the $TbPc_2$ molecules on the CNT were aligned in a parallel arrangement – ferromagnetic coupling – a maximum conductance was observed. In contrast, minimal conductance was obtained when the electron spin of the $TbPc_2$ was antiparallel – antiferromagnetic arrangement. The sensitivity of the tests revealed molecules bound to the CNT in various orientations. The nuclear spin transitions were obtained by determining the likelihood of tunneling as a function of sweep rate. When two $TbPc_2$ molecules were suspended on the CNT a spin-valve behaviour was observed. Below 1 K, a magnetoresistance of up to 300% was determined, suggesting that a greater number of molecules on the CNT were being individually controlled by a local gate. This would make it possible to use sophisticated quantum computing protocols. Remarkably, QTM suppression was determined when the $TbPc_2$ was suspended on a CNT, due to one-dimensional phonons connected to

the mechanical motion of the CNT,[92] enabling relaxation to proceed only through direct relaxation. In principle, the quantum Einstein-de Hass effect would provide coherent spin manipulation of the spin states, creating the potential for entanglement.[92]

Despite successful instances and the incorporation of single magnetic molecules into hybrid spintronic devices, the integration of a single magnetic molecule into such architectures remains a notable challenge. This integration faces two main obstacles: ensuring compatibility between the processing steps of the assemblies and the device, and precisely placing the molecular assemblies within the device. Strategies to address these challenges include fabricating the junction around the MM and/or selectively functionalizing MMs with anchoring groups (such as π-stacking-promoting moieties, sulfur, or oxygen) to guide their placement in the devices to the precise location.

4. Quantum Technologies Employing MMs

MMs have been shown to fulfill the so-called DiVincenzo criteria[93] to act as qubits. Due to the facile manipulation of the electronic spins, these have been proposed as electron and nuclear spin qubits whereby through the application of external stimuli they can be manipulated. Multilevel systems, also known as qu*d*its, where the *d* stands for the multilevel character of the system, have gained much attention due to the possibility of employing their multilevel nature to perform complex algorithms in a single physical unit. Qu*d*its offer several advantages over qubits, such as d^N orthogonal states, allowing parallelization in a single unit with lower error rates compared to the qubits counterparts.[94–100] In qu*d*its, the higher energy states can be used to execute complex quantum gates, among others.

Due to these characteristics, MMs have been proposed in several technological applications, including quantum sensing and quantum computing. Additionally, these systems may be successfully incorporated in spin-transistor and spin-valve devices, opening the door to hybrid quantum device designs. In the following section, some crucial requirements of MMs for each application are briefly described, as well as some experimental works.

4.1. Quantum Sensing

Quantum phenomena form the foundation of cutting-edge technologies, striving to achieve feats beyond the capabilities of classical systems. Quantum sensing, often known as Q-sensing, is an example of how quantum effects are used and exploited in sensing protocols. As shown by the discovery of gravitational waves using squeezed states of light made by the Advanced Light Interferometer Gravity-Wave Observatory (aLIGO),[101] it is conceivable to examine exceedingly minute fluctuations or disturbances using the sensitivity of quantum states.

At the core of Q-sensing are two crucial characteristics—quantum coherence and entanglement—which are the foundation for the development of Q-sensing.[102–104] Well-defined levels and the ability to initialize and read out the end state are likewise important. In certain situations, coherent manipulation of the states of the system becomes essential. Unlike the fundamental qubit in quantum computers, the Q-sensor must interact with the system under study. Specifically, the probe must be prepared in a state that depends on the parameter being measured. The ultimate result of the measurement may then be extrapolated from the interaction between the Q-sensor and the systems to be sensed, which results in some change in the initial characteristics of the sensor. Two alternative configurations can be formulated based on the interaction between the sensor and the system to be sensed: *i*) In the first setup, the sensor is ready in an initial state ρ_0, allowing contact with the system to be sensed or field under examination. The system that is being studied has an unknown parameter γ. Following the interaction of the sensor with the system being studied, the quantum probe measures γ. Ultimately, the information can be extracted using sensor measurements. *ii*) In the second arrangement, a quantum probe is included within a bigger structure, and its state provides details about the internal characteristics under study.

The benefits of quantum sensors depend largely on their ability to use quantum phenomena like entanglement and the superposition of states, making it possible to sense phenomena not detectable by conventional sensors. Several systems are being actively investigated as Q-sensors, including NV centers,[2–9,107,108] superconducting circuits,[103] light,[1,101,109] silicon vacancies,[110,111] and nuclear and electronic spins embedded in magnetic molecules,[102,104] among others. Due to their superior spatial resolution single atoms and molecules have quantum characteristics better suited to perform than any classical sensor for sensing at the nanometer scale.[102,104] Furthermore, precise chemical manipulation of their synthetic components allows for tailoring the structural, electrical, and nuclear characteristics of these systems. The long coherence times have made magnetic molecules proposed systems act as Q-sensors for the detection of physical properties including temperature, electrical or magnetic fields, currents, nuclear spins, electronic spins, and magnons to dark matter.[102,104] Additionally, by using interactions, chemically tailored design makes it easy to place sensors in the desired locations.

An example of a molecular system acting as a Q-sensor is a single $TbPc_2$ molecule serving as a local thermometer in a transistor arrangement.[112] The $TbPc_2$ molecule is connected to a magnetic field and is in thermal equilibrium, operating as a temperature sensor. After the application of non-resonant microwave pulses, it was discovered by electrical read-out and monitoring of the spin-flip of the electronic spin of the Tb^{3+} ion that the spin-flip rate follows an exponential rule, operating as a thermometer. Furthermore, Serrano and Sessoli demonstrated that a monolayer of $TbPc_2$ units on a superconducting Pb(111) surface functions as a sensor for topological hysteresis in superconductors[105] (**Figure 4A**). The topological hysteresis of the substrate, influenced by an external magnetic field, leads to localized changes in the magnetization of the $TbPc_2$ molecules within the monolayer. X-ray magnetic Circular Dichroism (XMCD) studies of the monolayer of $TbPc_2$ onto Pb(111) are found to be highly sensitive to the topology of the superconductor (Figure 4B,C). Decreasing the magnetic field below the critical field of the superconductor ($|H_C^{Pb}|$= 0.072 T), the XMCD signal of $TbPc_2$ that the magnetic field is only partially screened by the superconductor (Figure 4B,C). Crossing zero field and upon increasing fields the XMCD intensity goes down to zero until reaching a field value of $|H_C^{Pb}|$= 0.055 T. This behaviour highlights the total screening

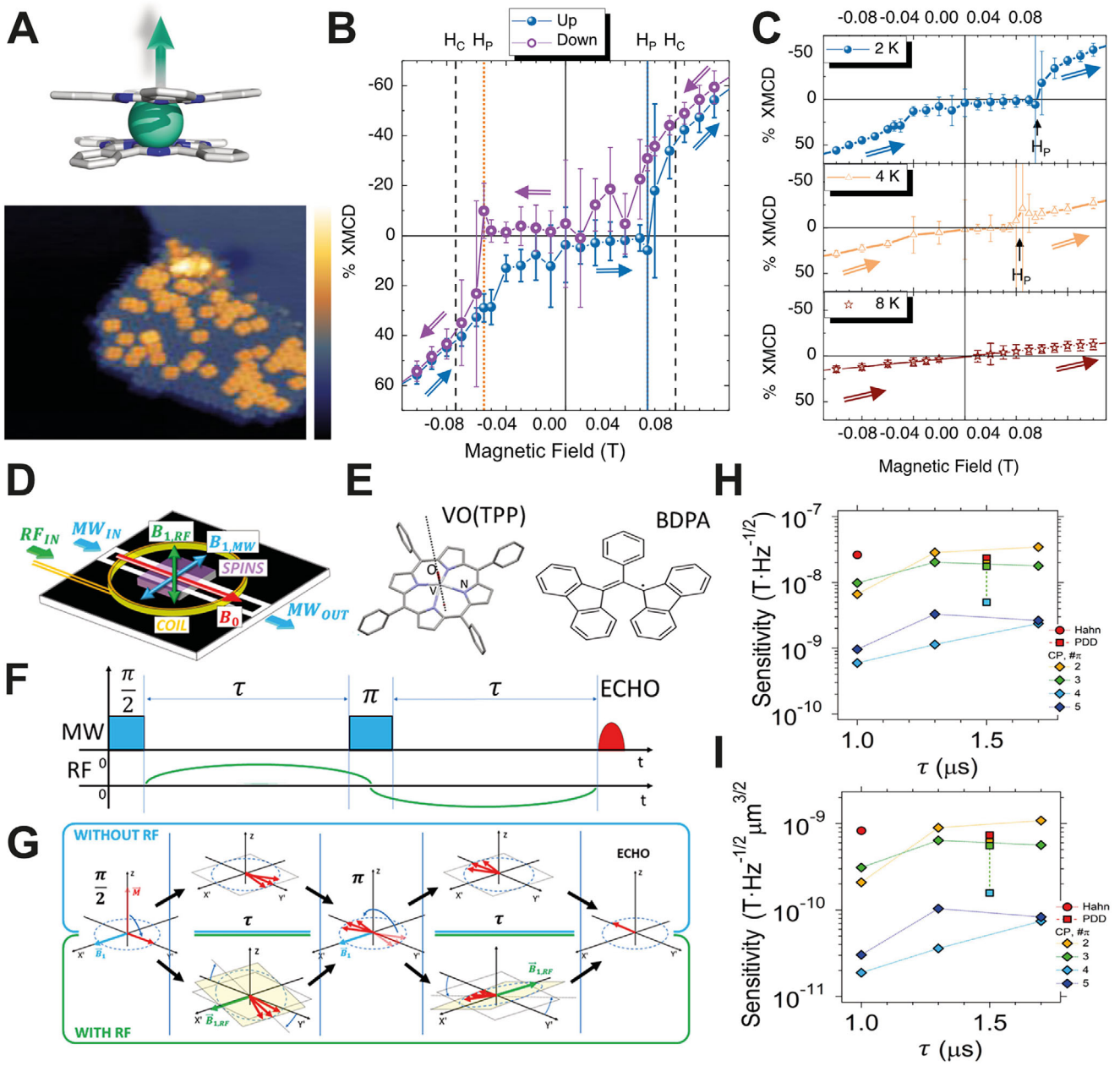

Figure 4. Quantum Sensing with Molecular Magnets: A) Molecular structure of the $TbPc_2$ MM. Color code: C, grey; N, blue; Tb, cyan. H omitted for clarity. The arrow represents the easy axis of the magnetization perpendicular to the Pc planes. B) XMCD magnetization curves of $TbPc_2$ monolayer onto Pb(111) at 2 K and $\theta = 0°$ within the critical field of the superconductor (H_C). The magnetic field screening effect of Pb is observed for increasing magnetic field intensity within a certain field H_P. C) Magnetisation curve (up sweep) of $TbPc_2$ on Pb(111) for $\theta = 0°$ at different temperatures below (2 and 4K) and above (8 K) $T_C = 7.2$ K. D) Coplanar resonator schematics with the MM (purple) and the radiofrequency (RF) coil (orange). The colored arrows represent the orientations of the static magnetic field (B_0), the microwave (MW) field (B_1, MW), and the RF field (B_1, RF). E) Structure diagram of VO(TPP) (left) and radical BDPA (right) used in the sensing scheme. F) Pulse sequence diagram employed for the quantum sensing protocol. G) Representation of the precession of the spins in the rotating reference frame during the application of pulse sequence shown in (F), with (bottom) or without (top) the application of the RF field. H) Experimental sensitivity of the quantum sensing protocol employing Dynamical Decoupling protocols on BDPA sample and its corresponding Sensitivity per unit of concentration I). Panels (A-C) adapted from ref. [105] CC-BY 4.0 International License, Springer Nature Copyright 2022. Panels (D-I) adapted from ref. [106] and CC-BY 4.0 International License, Springer Nature Copyright 2024.

of the magnetic field by the Pb(111) substrate below $|H_C^{Pb}|$. Consequently, this MM becomes highly sensitive to variations in the local magnetic field, making MMs highly susceptible sensors for superconductors.

Recently, Bonizzoni et al. demonstrated that quantum sensing protocols for AC magnetic fields can be implemented using molecular spin ensembles embedded in hybrid quantum circuits.[106] The study employed an oxovanadium (IV) tetraphenyl porphyrin (VO(TPP)), and an organic radical, namely the α, γ-bisdiphenylene-β-phenylally (BDPA), as prototypes (Figure 4D). By employing Dynamical Decoupling protocols synchronized with the AC magnetic fields, it was possible to achieve enhanced sensitivity up to 10^{-10} T $Hz^{-1/2}$ using only echo detection at microwave frequencies and no optical readout (Figure 4E).[106] This advancement opens new possibilities for probing magnetic fields at the atomic scale, which are not accessible by classical sensors.

Other local sensing protocols are based on a Spin-polarized Scanning Tunnelling Microscope (SP-STM)[113,114] in conjunction with electromagnetic pulses.[102] The Q-sensing approach involves applying a microwave pulse that causes an electronic transition, altering the population of the center, and then detecting that change with the SP-STM tip.[115–121] It has also been demonstrated that a $TbPc_2$ system's electronic and nuclear spin characteristics may be determined using an equivalent procedure.[102]

4.2. Quantum Information Processing

Richard Feynman asserted that quantum systems would be able to reproduce quantum effects in the early 1980s, stressing the shortcomings of classical computers.[10] Later, Shor,[122] Grover,[123] Lloyds,[11] and others supported Feynman's proposal after demonstrating that a quantum computer would have unmatched benefits over conventional computers.

Magnetic molecules have been shown to collect all the attributes required for qubits, i.e., *i*) well-defined states; *ii*) long coherence; *iii*) initialization of the system in well-defined states; *iv*) entanglement and/or superposition of states; *v*) read-out of the quantum states. They have been proposed as electron spin qubits due to the ease with which the electronic spins may be manipulated by applying external stimuli such as temperature, magnetic fields, or electromagnetic pulses.[19,124] Electron Paramagnetic Resonance (EPR) pulses are one of the suggested techniques for manipulating the electronic spins of magnetic molecules. EPR pulses may be used to control electron spin qubits, such as in the antiferromagnetic $\{Cr_7Ni\}$ wheels, systems that have shown long coherence times and great tunability of their properties. The wheel's Cr^{3+} and Ni^{2+} exhibit significant antiferromagnetic coupling, which creates a well-defined spin $S = 1/2$ ground state that is separated from excited states below 10 K.[124] Lanthanide-based magnetic molecules have also been proposed as qubits.[75,125,126] The concept of a CNOT gate was proposed because of the observation of a small interaction between the lanthanide ions Ce^{3+} and Er^{3+} in an asymmetric lanthanide dimer. Theoretically, it was proposed that the spin of the ions could be addressed by tuning the resonance frequencies or fields.[125]

The possibility of chemically modifying the structural and electronic characteristics of magnetic molecules makes it possible to bring two or more units, with the desired characteristics, into proximity. This is an important characteristic to create quantum gates for the implementation of quantum operations. MMs having a switchable linker between the two units have been proposed for quantum simulations, as theoretically exemplified by the $\{Cr_7Ni\}$ dimers to model quantum gates.[62,127,128] Atzori and colleagues likewise proposed, based on experimental parameters, a crucial instance of quantum simulation utilizing a molecular system.[129] A dimeric V^{4+} combination with the formula $[PPh_4]_4[(VO)_2(L_1)_2]$ was employed in the demonstration. Utilizing both the electronic and nuclear spins, (L_1 = tetraanion of $C_6H_3(OH)_2$-CONH-C_6H_4-CONH-$C_6H_3(OH)_2$). In the dimer, the electronic and nuclear states are connected by a hyperfine interaction, whereas the electronic spins of the V^{4+} are related through an exchange interaction, allowing the execution of a controlled shift (Cφ) two-qubit gate. This gate induces entanglement between the qubits and adds a phase to one of the states while leaving the other states unchanged. Ultimately, it was possible to accurately replicate the QTM of an $S = 1$ state using this system as a quantum simulator.[129]

Additionally, the multilevel nature of magnetic molecules may be taken as an advantage by using the excited levels as qubit units.[19,94–100] A molecular qu*d*it, composed of 2 spins, namely an $S = 1/2$ and $S \geq 3/2$ spins, has been suggested as a quantum simulator for light-matter interactions.[130] Likewise, using a gadolinium polyoxometalate complex with the formula $K_{12}Gd(H_2O)P_5W_{30}O_{110}{\cdot}27.5H_2O$ (GdW_{30}), the first manipulation of the electronic states in a qu*d*it was shown.[131,132] According to EPR studies, the huge spin multiplicity, $S = 7/2$, with a small, but significant anisotropy guarantees 8 potential states for manipulation. For the GdW_{30} complex, T_2 values between 400 and 600 ns and T_1 values between 2.3 and 2.8 µs were reported. Employing the GdW_{30} a controlled-controlled-NOT (CCNOT) or Toffoli gate was performed, illustrating the benefits of multilevel systems. As an extension of the single Gd^{3+} qudit example, an asymmetric dimeric gadolinium dinuclear system has also been characterized and considered to act as qu*d*it, with a Hilbert space of $d = 64$, in principle, allowing the execution of more advanced algorithms.[133]

Although using the electronic spin in magnetic molecules as qubits is being investigated, the electron spin is particularly vulnerable to interactions with the spin bath.[134] The $TbPc_2$ molecule is a prime example of a nuclear spin qu*d*it, in which a quantum algorithm has been experimentally realized at a single molecule level. The execution of Grover's quantum algorithm employing multilevel systems was first proposed by Lebenwauer and Loss, taking advantage of the 21-level manifold of Fe_8 and Mn_{12}. However, it was just until 2017 that the execution of this algorithm was realized in MM. Through an indirect interaction between the electronic spin and nuclear spin via the hyperfine interaction, read-out of the nuclear states is achievable. The initialization of the nuclear states is accomplished at sub-kelvin temperatures and low applied fields, which corresponds to the 4 nuclear qu*d*its states, namely $|m_I = \pm 1/2\rangle$ and $|m_I = \pm 3/2\rangle$.[82,84] Manipulation of these states is possible by using pulse sequences that correspond to the uneven separation between the states caused by the quadrupolar interaction (**Figure 5**A).[36] Following the superposition of state employing a Hadamard gate, the frequencies, and amplitudes, are tuned to

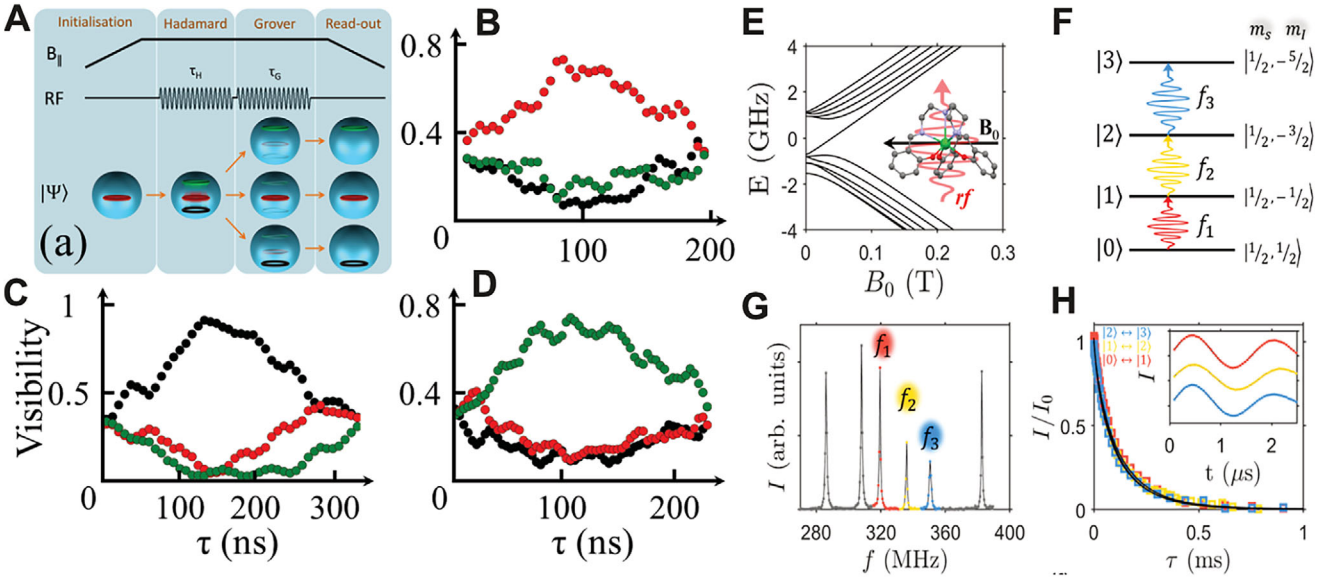

Figure 5. Quantum Computing with Qu*d*its: A) Grover algorithm is implemented using 4 different steps: initialization, Hadamard gate, Grover gate, and final read-out; B) Grover evolution. Dynamic of the population as a function of the unitary evolution pulse length. Starting from a superposition of 3 states, generated through a Hadamard gate, an oscillation between this superposed state and a desired state is created. Depending on the detuning sequence, the population from $|-1/2\rangle$ (B), $|-3/2\rangle$ C) or a $|+1/2\rangle$ D) state increases. E) Energy level diagram of ^{173}Yb(trensal) with the static field B_0 perpendicular to the molecular C_3 axis; F) Schematic representation of the nuclear qu*d*it; G) NMR spectrum of the ^{173}Yb(trensal) qu*d*it at $B_0 = 0.12$ T and $T = 1.4$ K, with the peaks representing the nuclear transitions within the computational subspace; H) Relaxation times T_1^{η} measured (dots) on each of the nuclear transitions with the multifrequency protocol, and some examples of coherent Rabi manipulation of the transitions indicated in panel (F) (Inset), demonstrating universal qu*d*it control. Panels (A) and (B) adapted from ref. [19] with permission from the Royal Society of Chemistry. Panels (E-H) adapted from ref. [135] CC-BY 4.0, Copyright 2023 The Authors. Published by American Chemical Society.

reach a resonance condition in between the superposed states and the sought state. As a result, the qu*d*it populations start to oscillate and the population of the labeled state briefly increases (Figure 5B–D). Long T_1 and T_2 values have also been attained for these systems, which, along with the capacity to read out, initialize, and alter nuclear states, enabled the implementation of Grover's algorithm. These results highlight the importance of the exploitation of the multilevel character of MMs to carry out complex algorithms in a single molecule. Naturally, for the execution of more complex algorithms, a larger number of accessible excited states and individually addressable estates are desired.

Inherently, for the execution of more complex algorithms, the Hilbert scale of MMs must be expanded, as well as maintaining the number of states individually accessible. An alternative reminiscent of the nuclear spin qu*d*it scheme in $TbPc_2$, electron-nuclear multilevel electron-nuclear MMs has also been proposed for quantum simulators.[129,130,136] The electronic states, coupled to the nuclear state by a hyperfine interaction, can act as quantum registers in these systems. To this end, V^{4+}-based complexes, taking advantage of the $I = 7/2$, have been explored leading to coherent manipulation of the nuclear states embedded in the molecule.[137,138] A second approach is based on isotopological chemistry, whereby by isotopically enriched metal sources, large spin multiplicities can be achieved. An example of such an approach is the ^{173}Yb(trensal) complex ($I = 5/2$).[135] This system serves as the first proof-of-concept experimental demonstration of a quantum simulation employing a molecular spin qu*d*it. Employing the nuclear states of ^{173}Yb(trensal), it was possible to simulate the QTM and the transverse-field Ising model in a single unit, demonstrating the versatility of qu*d*its to execute quantum algorithms.

In all the aforementioned cases, the different accessible states can be utilized to perform quantum algorithms or quantum simulations. However, a major problem for any qubit platform is the correction of errors occurring during the computational execution. In this sense, MMs have also been proposed to encrypt and safeguard the qubit using Quantum Error Correction (QEC) protocols due to their multilayer properties at the electronic and nuclear levels.[24–28] Being able to shield quantum information from decoherent sources and quantum noise is crucial for the successful implementation of quantum computing. As a result, QEC, which may lessen mistakes caused by noise, quantum gate faults, incorrect initialization, and manipulation of the data and measurements, is crucial for the development of fault-tolerant universal quantum computing. The "logical qubits" used in QEC schemes are systems with more than 2 levels; these qubits place the system in a specified state outside the computational domain, allowing for the detection and correction of faults. However, this strategy has certain challenges since QEC and quantum computation need non-local states in separate objects. Encoding the logical qubit into a single qu*d*it object is an alternate method, exploiting ancillary states (**Figure** 6A,B). Subsequent projection of the states allows the restoration of the error-corrected original state (**Figure** 6D).[28,136]

gMMs have likewise been proposed for QEC protocols. The key ingredients for the implementation of MMs as QEC registers have been described in detail by Carretta and co-workers, including a hypothetical case whereby the antiferromagnetic

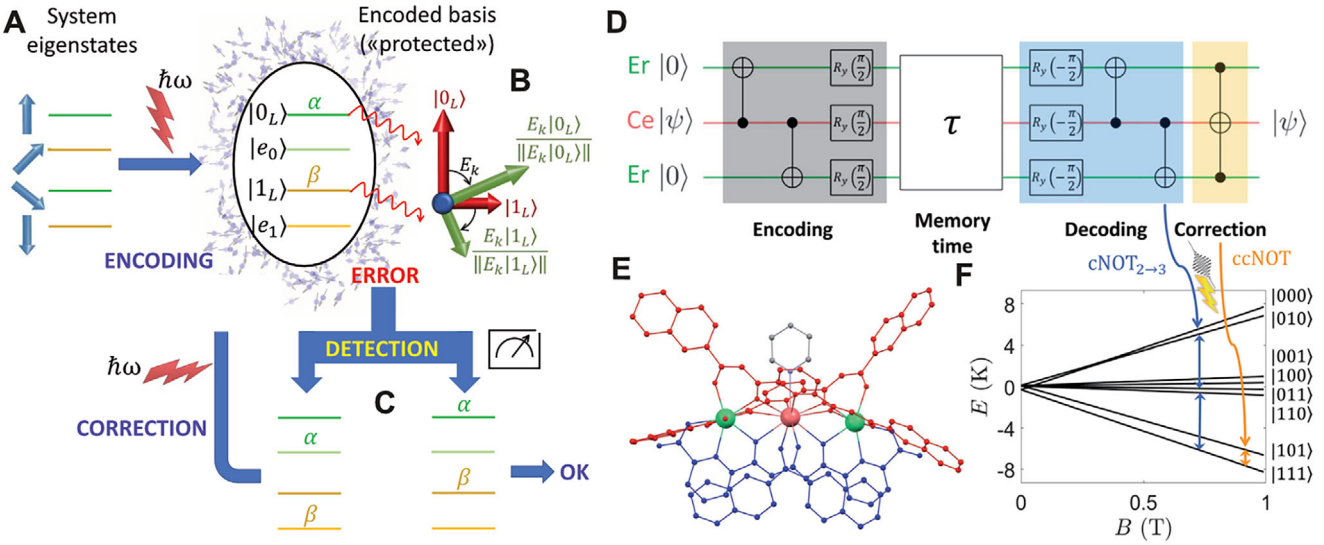

Figure 6. Quantum Error Correction: A) Schematic representation of QEC schemes implemented in qu*d*it ($d = 4$). By exploiting the resonance frequencies, the information can be encoded into a combination of eigenstates protected from errors B); C) projection of the state of the system allows the restoration of the error-corrected original state; D) Quantum circuit for a three-qubit phase-flip repetition code. The central qubit carries the information, while the remaining are auxiliary qubits; E) The molecular structure of *f*-SMM (Er, green, and Ce, light red) corresponds to the qubits of the circuit shown in (D); F) Energy levels as a function of the external field *B* applied along *z* (the Er–Ce direction). Panels (A-C) from Ref[136] CC-BY 3.0, IOP Publishing Nature Copyright 2024. Panels (D-F) adapted from ref. [27] CC-BY 3.0, Royal Society of Chemistry.

coupling between the ions renders many low-lying, resilient to decoherence, energy states.[28] At a molecular level, a heterometallic trinuclear [ErCeEr] trinuclear complex, with an interaction linking the Er-Ce pair has been proposed for QEC schemes (Figure 5A,B).[27] Numerical simulation shows that the complex may be used to protect qubits against single-bit or phase-flip errors in a three-qubit repetition code (Figure 5C). The steps in the correction process include encoding, decoding, and correction. Two controlled-NOT (cNOT) two-qubit gates induce a flip on the target qubit—which is shielded from error by entanglement—during the encoding process. The qubit is kept in the memory, and the decoding (reverse encoding) is done later. Correction may eventually be performed to the qubit using a single controlled-controlled-NOT (ccNOT) gate, effectively the qubit from decoherence.

The Cr_7Ni-Cu system has also been proposed for QEC schemes, where the electronic state of the Cr_7Ni and the nuclear state contained in the Cu^{2+} ion may be utilized.[26] Complex quantum algorithms need extensive periods of inactivity during which the qubits sit dormant in between sets of quantum operations. Therefore, it is possible to use the nuclear spins buried in Cu^{2+} as a quantum memory to store data when needed. Information may be secured for a lot longer than processor coherence by making use of the nuclear states in Cu^{2+} that operate as storage states with quantum error correction. These examples undoubtedly opened the path for MMs for all-encompassing fault-tolerant quantum computer architectures.[25]

5. Conclusion and Outlook

MMs have been the focus of several investigations since the early 1990s when the barrier to the relaxation to magnetization was discovered. Since then, these systems have been shown to possess several quantum effects, making them nice prospects for quantum technologies. A salient feature of MMs is the possibility of engineering their structural and electronic character to a large extent. Furthermore, these nanometric size systems are highly reproducible, which along with the tailored character, make them natural prospects for new technologies. A thorough understanding of the characteristics of these systems has led to the development of SMMs that operate above liquid nitrogen temperatures,[44] systems with remarkably long coherence times,[66–73] and the integration and manipulation of their quantum states.[36] These salient features make them strong candidates as quantum sensors, quantum simulators to the basic units of quantum computers. Quantum sensing capabilities have been observed for a monolayer of $TbPc_2$ onto a superconducting surface, revealing high sensitivity to the topology of the superconductor.[105] Similarly, enhanced sensitivities up to $S \approx 10^{-10}$–10^{-9} T $Hz^{-1/2}$ with low pulse numbers have been achieved using MMs.[106]

Furthermore, due to the control over the structural, but also nuclear and electronic characteristics, MMs have been proposed as qu*d*it. Qu*d*its are more suitable candidates for quantum computing due to the possibility of exploiting the ancillary states to execute quantum algorithms, quantum gates, and integrated quantum error correction protocols. Proof-of-concept examples are the execution of a quantum algorithm in a single $TbPc_2$ unit,[36] quantum simulation employing ^{173}Yb(trensal)[135] crystals, and quantum error corrections in a [ErCeEr] trinuclear complex.[27] In all cases, the possibility of creating multilevel systems with different energy spacing between the levels opens the possibility of manipulation of the individual states employing pulse sequences and the execution of complex operations in a single entity. For the successful incorporation of these bewildering objects in single-molecule quantum technologies, nevertheless, a main challenge

is their integration into hybrid devices. Several strategies are envisioned to overcome this challenge. From the chemical perspective, MMs with tailored functions might allow the integration of the molecule into specific locations of the devices, whilst at the device side, fabricating the junction around the molecule are alternative. An alternative strategy is concerned with the exploitation of the molecular assembly character of MMs to carry out quantum algorithms, exploiting broad-band EPR or NMR experiments on crystals coupled to superconducting cavities.[136–141] In all cases, the very reliable control over MMs allows the design of the desired characteristics of these nano-objects.

To bring more investigation into these systems, we have shown some key characteristics that make these systems promising building blocks for quantum technologies. The integration of MMs into hybrid quantum devices has been demonstrated, however, a larger effort is required of the community to test the myriads of molecular systems that are continuously synthesized and to develop further the field.

Acknowledgements

W.W. thanks the German Research Foundation (DFG) for the Gottfried Wilhelm Leibniz-Award, ZVN-2020_WE 4458-5. E.M.-P. thanks to the Alexander von Humboldt fellowship for experienced researchers for support.

Open access funding enabled and organized by Projekt DEAL.

Conflict of Interest

The authors declare no conflict of interest.

Keywords

magnetic molecules, quantum information processing, qudit, single-molecule magnet

Received: October 18, 2023
Revised: October 15, 2024
Published online: October 30, 2024

[1] B. J. Lawrie, P. D. Lett, A. M. Marino, R. C. Pooser, *ACS Photonics* **2019**, *6*, 1307.
[2] V. Radu, J. C. Price, S. J. Levett, K. K. Narayanasamy, T. D. Bateman-Price, P. B. Wilson, M. L. Mather, *ACS Sens.* **2020**, *5*, 703.
[3] E. Lee-Wong, R. Xue, F. Ye, A. Kreisel, T. Van Der Sar, A. Yacoby, C. R. Du, *Nano Lett.* **2020**, *20*, 3284.
[4] A. Jenkins, M. Pelliccione, G. Yu, X. Ma, X. Li, K. L. Wang, A. C. B. Jayich, *Phys. Rev. Mater.* **2019**, *3*, 83801.
[5] J. F. Barry, M. J. Turner, J. M. Schloss, D. R. Glenn, Y. Song, M. D. Lukin, H. Park, R. L. Walsworth, *Proc. Natl. Acad. Sci. U.S.A.* **2016**, *113*, 14133.
[6] Y. Dovzhenko, F. Casola, S. Schlotter, T. X. Zhou, F. Büttner, R. L. Walsworth, G. S. D. Beach, A. Yacoby, *Nat. Commun.* **2018**, *9*, 2712.
[7] J. M. Boss, K. S. Cujia, J. Zopes, C. L. Degen, *Science* **2017**, *356*, 837.
[8] F. Shi, Q. Zhang, P. Wang, H. Sun, J. Wang, X. Rong, M. Chen, C. Ju, F. Reinhard, H. Chen, J. Wrachtrup, J. Wang, J. Du, *Science* **2015**, *347*, 1135.
[9] I. Lovchinsky, A. O. Sushkov, E. Urbach, N. P. de Leon, S. Choi, K. De Greve, R. Evans, R. Gertner, E. Bersin, C. Müller, L. McGuinness, F. Jelezko, R. L. Walsworth, H. Park, M. D. Lukin, *Science* **2016**, *351*, 836.
[10] R. P. Feynman, *Int. J. Theoretical Phys.* **1982**, *21*, 467.
[11] S. Lloyd, *Science* **1993**, *261*, 1569.
[12] S. Lloyd, *Science* **1996**, *273*, 1073.
[13] G. García-Pérez, M. A. C. Rossi, S. Maniscalco, *npj Quantum Inf.* **2020**, *6*, 1.
[14] J. Kelly, R. Barends, A. G. Fowler, A. Megrant, E. Jeffrey, T. C. White, D. Sank, J. Y. Mutus, B. Campbell, Y. Chen, Z. Chen, B. Chiaro, A. Dunsworth, I.-C. Hoi, C. Neill, P. J. J. O'Malley, C. Quintana, P. Roushan, A. Vainsencher, J. Wenner, A. N. Cleland, J. M. Martinis, *Nature* **2015**, *519*, 66.
[15] T. F. Watson, S. G. J. Philips, E. Kawakami, D. R. Ward, P. Scarlino, M. Veldhorst, D. E. Savage, M. G. Lagally, M. Friesen, S. N. Coppersmith, M. A. Eriksson, L. M. K. Vandersypen, *Nature* **2018**, *555*, 633.
[16] F. Arute, K. Arya, R. Babbush, D. Bacon, J C. Bardin, R. Barends, R. Biswas, S. Boixo, F G. S. L. Brandao, D A. Buell, B. Burkett, Yu Chen, Z. Chen, B. Chiaro, R. Collins, W. Courtney, A. Dunsworth, E. Farhi, B. Foxen, A. Fowler, C. Gidney, M. Giustina, R. Graff, K. Guerin, S. Habegger, M P. Harrigan, M J. Hartmann, A. Ho, M. Hoffmann, T. Huang, et al., *Nature* **2019**, *574*, 505.
[17] M. Atzori, R. Sessoli, *J. Am. Chem. Soc.* **2019**, *141*, 11339.
[18] W. Wernsdorfer, M. Ruben, *Adv. Mater.* **2019**, 31, https://doi.org/10.1002/adma.201806687.
[19] E. Moreno-Pineda, C. Godfrin, F. Balestro, W. Wernsdorfer, M. Ruben, *Chem. Soc. Rev.* **2018**, *47*, 501.
[20] A. Gaita-Ariño, F. Luis, S. Hill, E. Coronado, *Nat. Chem.* **2019**, *11*, 301.
[21] J. J. Pla, K. Y. Tan, J. P. Dehollain, W. H. Lim, J. J. L. Morton, D. N. Jamieson, A. S. Dzurak, A. Morello, *Nature* **2012**, *489*, 541.
[22] D. Loss, D. P. DiVincenzo, *Phys. Rev. A.* **1998**, *57*, 120.
[23] S. Carretta, D. Zueco, A. Chiesa, Gómez-León, F. L, *Appl. Phys. Lett.* **2021**, *118*, 1.
[24] M. Chizzini, L. Crippa, L. Zaccardi, E. Macaluso, S. Carretta, A. Chiesa, P. Santini, *Phys. Chem. Chem. Phys.* **2022**, *24*, 20030.
[25] A. Chiesa, E. Macaluso, F. Petiziol, S. Wimberger, P. Santini, S. Carretta, *J. Phys. Chem. Lett.* **2020**, *11*, 8610.
[26] S. J. Lockyer, A. Chiesa, G. A. Timco, E. J. L. McInnes, T. S. Bennett, I. J. Vitorica-Yrezebal, S. Carretta, R. E. P. Winpenny, *Chem. Sci.* **2021**, *12*, 9104.
[27] E. Macaluso, M. Rubín, D. Aguilà, A. Chiesa, L. A. Barrios, J. I. Martínez, P. J. Alonso, O. Roubeau, F. Luis, G. Aromí, S. Carretta, *Chem. Sci.* **2020**, *11*, 10337.
[28] A. Chiesa, F. Petiziol, M. Chizzini, P. Santini, S. Carretta, *J. Phys. Chem. Lett.* **2022**, *13*, 6468.
[29] R. Sessoli, D. Gatteschi, A. Caneschi, M. A. Novak, *Nature* **1993**, *365*, 141.
[30] N. E. Chakov, S. C. Lee, A. G. Harter, P. L. Kuhns, A. P. Reyes, S. O. Hill, N. S. Dalal, W. Wernsdorfer, K. A. Abboud, G. Christou, *J. Am. Chem. Soc.* **2006**, *128*, 6975.
[31] J. R. Friedman, M. P. Sarachik, J. Tejada, R. Ziolo, *Phys. Rev. Lett.* **1996**, *76*, 3830.
[32] N. Ishikawa, M. Sugita, T. Ishikawa, S. Y. Koshihara, Y. Kaizu, *J. Am. Chem. Soc.* **2003**, *125*, 8694.
[33] N. Ishikawa, M. Sugita, T. Okubo, N. Tanaka, T. Iino, Y. Kaizu, *Inorg. Chem.* **2003**, *42*, 2440.
[34] N. Ishikawa, M. Sugita, W. Wernsdorfer, *Angewandte Chemie – Int. Ed.* **2005**, *44*, 2931.
[35] N. Ishikawa, M. Sugita, W. Wernsdorfer, *J. Am. Chem. Soc.* **2005**, *127*, 3650.
[36] C. Godfrin, A. Ferhat, R. Ballou, S. Klyatskaya, M. Ruben, W. Wernsdorfer, F. Balestro, *Phys. Rev. Lett.* **2017**, *119*, 187702.
[37] N. F. Chilton, *Inorg. Chem.* **2015**, *54*, 2097.
[38] J. G. C. Kragskow, A. Mattioni, J. K. Staab, D. Reta, J. M. Skelton, N. F. Chilton, *Chem. Soc. Rev.* **2023**, *52*, 4567.

[39] W. Zhang, A. Muhtadi, N. Iwahara, L. Ungur, L. F. Chibotaru, *Angewandte Chemie – Int. Ed.* **2020**, *59*, 12720.
[40] P. B. Jin, Q. C. Luo, G. K. Gransbury, I. J. Vitorica-Yrezabal, T. Hajdu, I. Strashnov, E. J. L. McInnes, R. E. P. Winpenny, N. F. Chilton, D. P. Mills, Y. Z. Zheng, *J. Am. Chem. Soc.* **2023**, *145*, 27993.
[41] A. H. Vincent, Y. L. Whyatt, N. F. Chilton, J. R. Long, *J. Am. Chem. Soc.* **2023**, *145*, 1572.
[42] C. A. P. Goodwin, F. Ortu, D. Reta, N. F. Chilton, D. P. Mills, *Nature* **2017**, *548*, 439.
[43] C. A. Gould, K. R. McClain, D. Reta, J. G. C. Kragskow, D. A. Marchiori, E. Lachman, E. Choi, J. G. Analytis, R. D. Britt, N. F. Chilton, B. G. Harvey, J. R. Long, *Science* **2022**, *375*, 198.
[44] F. S. Guo, B. M. Day, Y. C. Chen, M. L. Tong, A. Mansikkamäki, R. A. Layfield, *Science* **2018**, *362*, 1400.
[45] H. Kwon, K. R. McClain, J. G. C. Kragskow, J. K. Staab, M. Ozerov, K. R. Meihaus, B. G. Harvey, E. S. Choi, N. F. Chilton, J. R. Long, *J. Am. Chem. Soc.* **2024**, *146*, 18714.
[46] M. Briganti, F. Santanni, L. Tesi, F. Totti, R. Sessoli, A. Lunghi, *J. Am. Chem. Soc.* **2021**, *143*, 13633.
[47] F. Santanni, A. Albino, M. Atzori, D. Ranieri, E. Salvadori, M. Chiesa, A. Lunghi, A. Bencini, L. Sorace, F. Totti, R. Sessoli, *Inorg. Chem.* **2021**, *60*, 140.
[48] R. Mirzoyan, R. G. Hadt, *Phys. Chem. Chem. Phys.* **2020**, *22*, 11249.
[49] A. Albino, S. Benci, L. Tesi, M. Atzori, R. Torre, S. Sanvito, R. Sessoli, A. Lunghi, *Inorg. Chem.* **2019**, *58*, 10260.
[50] J. G. C. Kragskow, J. Marbey, C. D. Buch, J. Nehrkorn, M. Ozerov, S. Piligkos, S. Hill, N. F. Chilton, *Nat. Commun.* **2022**, *13*, 825.
[51] S. Mondal, A. Lunghi, *J. Am. Chem. Soc.* **2022**, *144*, 22965.
[52] A. Lunghi, S. Sanvito, *Sci. Adv.* **2019**, *5*, 1.
[53] A. Lunghi, F. Totti, R. Sessoli, S. Sanvito, *Nat. Commun.* **2017**, *8*, 1.
[54] A. Lunghi, *Sci. Adv.* **2022**, *8*, 7880.
[55] A. Mattioni, J. K. Staab, W. J. A. Blackmore, D. Reta, J. Iles-Smith, A. Nazir, N. F. Chilton, *Nat. Commun.* **2024**, *15*, https://doi.org/10.1038/s41467-023-44486-3.
[56] D. Gatteschi, R. Sessoli, *Angewandte Chemie – Int. Ed.* **2003**, *42*, 268.
[57] E. Moreno-Pineda, M. Damjanović, O. Fuhr, W. Wernsdorfer, M. Ruben, *Angewandte Chemie – Int. Ed.* **2017**, *56*, 9915.
[58] E. Moreno-Pineda, S. Klyatskaya, P. Du, M. Damjanović, G. Taran, W. Wernsdorfer, M. Ruben, *Inorg. Chem.* **2018**, *57*, 9873.
[59] H. Biard, E. Moreno-Pineda, M. Ruben, E. Bonet, W. Wernsdorfer, F. Balestro, *Nat. Commun.* **2021**, *12*, 4443.
[60] C. J. Wedge, G. A. Timco, E. T. Spielberg, R. E. George, F. Tuna, S. Rigby, E. J. L. McInnes, R. E. P. Winpenny, S. J. Blundell, A. Ardavan, *Phys. Rev. Lett.* **2012**, *108*, 107204.
[61] G. A. Timco, S. Carretta, F. Troiani, F. Tuna, R. J. Pritchard, C. A. Muryn, E. J. L. McInnes, A. Ghirri, A. Candini, P. Santini, G. Amoretti, M. Affronte, R. E. P. Winpenny, *Nat. Nanotechnol.* **2009**, *4*, 173.
[62] J. Ferrando-Soria, E. M Pineda, A. Chiesa, A. Fernandez, S. A. Magee, S. Carretta, P. Santini, I. J. Vitorica-Yrezabal, F. Tuna, G. A. Timco, E. J. L. McInnes, R. E. P. Winpenny, *Nat. Commun.* **2016**, *7*, 11377.
[63] A. Fernandez, E. M Pineda, C. A. Muryn, S. Sproules, F. Moro, G. A. Timco, E. J. L. McInnes, R. E. P. Winpenny, *Angewandte Chemie – Int. Ed.* **2015**, *54*, 10858.
[64] J. Ferrando-Soria, A. Fernandez, E. M Pineda, S. A. Varey, R. W. Adams, I. J. Vitorica-Yrezabal, F. Tuna, G. A. Timco, C. A. Muryn, R. E. P. Winpenny, *J. Am. Chem. Soc.* **2015**, *137*, 7644.
[65] K. Bader, D. Dengler, S. Lenz, B. Endeward, S. Da Jiang, P. Neugebauer, J. Van Slageren, *Nat. Commun.* **2014**, *5*, 5304.
[66] M. Atzori, L. Tesi, E. Morra, M. Chiesa, L. Sorace, R. Sessoli, *J. Am. Chem. Soc.* **2016**, *138*, 2154.
[67] C. J. Yu, M. J. Graham, J. M. Zadrozny, J. Niklas, M. D. Krzyaniak, M. R. Wasielewski, O. G. Poluektov, D. E. Freedman, *J. Am. Chem. Soc.* **2016**, *138*, 14678.
[68] M. J. Graham, J. M. Zadrozny, M. Shiddiq, J. S. Anderson, M. S. Fataftah, S. Hill, D. E. Freedman, *J. Am. Chem. Soc.* **2014**, *136*, 7623.
[69] M. S. Fataftah, J. M. Zadrozny, S. C. Coste, M. J. Graham, D. M. Rogers, D. E. Freedman, *J. Am. Chem. Soc.* **2016**, *138*, 1344.
[70] J. M. Zadrozny, J. Niklas, O. G. Poluektov, D. E. Freedman, *J. Am. Chem. Soc.* **2014**, *136*, 15841.
[71] M. Atzori, E. Morra, L. Tesi, A. Albino, M. Chiesa, L. Sorace, R. Sessoli, *J. Am. Chem. Soc.* **2016**, *138*, 11234.
[72] L. Tesi, E. Lucaccini, I. Cimatti, M. Perfetti, M. Mannini, M. Atzori, E. Morra, M. Chiesa, A. Caneschi, L. Sorace, R. Sessoli, *Chem. Sci.* **2016**, *7*, 2074.
[73] M. Atzori, L. Tesi, S. Benci, A. Lunghi, R. Righini, A. Taschin, R. Torre, L. Sorace, R. Sessoli, *J. Am. Chem. Soc.* **2017**, *139*, 4338.
[74] M. J. Graham, J. M. Zadrozny, M. S. Fataftah, D. E. Freedman, *Chem. Mater.* **2017**, *29*, 1885.
[75] M. Shiddiq, D. Komijani, Y. Duan, A. Gaita-Ariño, E. Coronado, S. Hill, *Nature* **2016**, *531*, 348.
[76] R. Stewart, A. B. Canaj, S. Liu, E. Regincós Martí, A. Celmina, G. Nichol, H. P. Cheng, M. Murrie, S. Hill, *J. Am. Chem. Soc.* **2024**, *146*, 11083.
[77] S. Giménez-Santamarina, S. Cardona-Serra, J. M. Clemente-Juan, A. Gaita-Ariño, E. Coronado, *Chem. Sci.* **2020**, *11*, 10718.
[78] K. Kundu, J. R. K. White, S. A. Moehring, J. M. Yu, J. W. Ziller, F. Furche, W. J. Evans, S. Hill, *Nat. Chem.* **2022**, *14*, 392.
[79] H. B. Heersche, Z. De Groot, J. A. Folk, H. S. J. Van Der Zant, C. Romeike, M. R. Wegewijs, L. Zobbi, D. Barreca, E. Tondello, A. Cornia, *Phys. Rev. Lett.* **2006**, *96*, 206801.
[80] J. F. Nossa, M. F. Islam, C. M. Canali, M. R. Pederson, *Phys. Rev. B Condens Matter Mater. Phys.* **2013**, *88*, 224423.
[81] R. Vincent, S. Klyatskaya, M. Ruben, W. Wernsdorfer, F. Balestro, *Nature* **2012**, *488*, 357.
[82] S. Thiele, R. Vincent, M. Holzmann, S. Klyatskaya, M. Ruben, F. Balestro, W. Wernsdorfer, *Phys. Rev. Lett.* **2013**, *111*, 037203.
[83] C. Godfrin, S. Thiele, A. Ferhat, S. Klyatskaya, M. Ruben, W. Wernsdorfer, F. Balestro, *ACS Nano* **2017**, *11*, 3984.
[84] S. Thiele, F. Balestro, R. Ballou, S. Klyatskaya, M. Ruben, W. Wernsdorfer, *Science* **2014**, *344*, 1135.
[85] C. Godfrin, R. Ballou, E. Bonet, M. Ruben, S. Klyatskaya, W. Wernsdorfer, F. Balestro, *npj Quantum Inf.* **2018**, *4*, 53.
[86] E. Moreno-Pineda, W. Wernsdorfer, *Nat. Rev. Phys.* **2021**, *3*, 645.
[87] M. Urdampilleta, S. Klyatskaya, J. P. Cleuziou, M. Ruben, W. Wernsdorfer, *Nat. Mater.* **2011**, *10*, 502.
[88] M. Urdampilleta, S. Klyatskaya, M. Ruben, W. Wernsdorfer, *Phys. Rev. B.* **2013**, *87*, 195412.
[89] M. Urdampilleta, S. Klayatskaya, M. Ruben, W. Wernsdorfer, *ACS Nano* **2015**, *9*, 4458.
[90] M. Ganzhorn, S. Klyatskaya, M. Ruben, W. Wernsdorfer, *Nat. Nanotechnol.* **2013**, *8*, 165.
[91] M. Ganzhorn, S. Klyatskaya, M. Ruben, W. Wernsdorfer, *ACS Nano* **2013**, *7*, 6225.
[92] M. Ganzhorn, S. Klyatskaya, M. Ruben, W. Wernsdorfer, *Nat. Commun.* **2016**, *7*, 11443.
[93] D. P. DiVincenzo, *Fortschritte der Physik* **2000**, *48*, 771.
[94] M. Mohammadi, A. Niknafs, M. Eshghi, *Quantum Inf. Process.* **2011**, *10*, 241.
[95] E. O. Kiktenko, A. K. Fedorov, A. A. Strakhov, V. I. Man'Ko, *Phys. Lett.* **2015**, *379*, 1409.
[96] D. P. O'Leary, G. K. Brennen, S. S. Bullock, *Phys. Rev. A.* **2006**, *74*, 032334.
[97] S. Balakrishnan, *Phys. Res. Int.* **2014**, *2014*, 1.
[98] A. Popov, E. Kiktenko, A. Fedorov, V. I. Man'ko, *J. Russ. Laser Res.* **2016**, *37*, 581.
[99] E. O. Kiktenko, A. K. Fedorov, O. V. Man'ko, V. I. Man'ko, *Phys. Rev. A.* **2015**, *91*, 042312.

[100] P. Rungta, W. J. Munro, K. Nemoto, P. Deuar, G. J. Milburn, C. M. Caves, *Direct. Quantum Optics* **2007**, 149.
[101] J. Aasi, J. Abadie, B. P. Abbott, R. Abbott, T. D. Abbott, M. R. Abernathy, C. Adams, T. Adams, P. Addesso, R. X. Adhikari, C. Affeldt, O. D. Aguiar, P. Ajith, B. Allen, E. Amador Ceron, D. Amariutei, S. B. Anderson, W. G. Anderson, K. Arai, M. C. Araya, C. Arceneaux, S. Ast, S. M. Aston, D. Atkinson, P. Aufmuth, C. Aulbert, L. Austin, B. E. Aylott, S. Babak, P. T. Baker, et al., *Nat. Photonics* **2013**, *7*, 613.
[102] F. Troiani, A. Ghirri, M. G. A. Paris, C. Bonizzoni, M. Affronte, *J. Magn. Magn. Mater.* **2019**, *491*, 165534.
[103] C. L. Degen, F. Reinhard, P. Cappellaro, *Rev. Mod. Phys.* **2017**, *89*, 035002.
[104] C. J. Yu, S. Von Kugelgen, D. W. Laorenza, D. E. Freedman, *ACS Cent. Sci.* **2021**, *7*, 712.
[105] G. Serrano, L. Poggini, G. Cucinotta, A. L. Sorrentino, N. Giaconi, B. Cortigiani, D. Longo, E. Otero, P. Sainctavit, A. Caneschi, M. Mannini, R. Sessoli, *Nat. Commun.* **2022**, *13*, https://doi.org/10.1038/s41467-022-31320-5.
[106] C. Bonizzoni, A. Ghirri, F. Santanni, M. Affronte, *npj Quantum Inf.* **2024**, *10*, https://doi.org/10.1038/s41534-024-00838-5.
[107] D. Kim, M. I. Ibrahim, C. Foy, M. E. Trusheim, R. Han, D. R. Englund, *Nat. Electron.* **2019**, *2*, 284.
[108] A. Cooper, W. K. C. Sun, J. C. Jaskula, P. Cappellaro, *Phys. Rev. Lett.* **2020**, *124*, 83602.
[109] K. P. Panajotov, M. Arizaleta, V. Gomez, K. Koltys, A. Tabaka, M. Sciamanna, I. Veretennicoff, H. Thienpont, *Quantum Sens. Nanophot. Dev.* **2004**, *5359*, 360.
[110] G. W. Morley, *Electron Paramagn. Reson.* **2015**, *24*, 62.
[111] T. Ohshima, T. Satoh, H. Kraus, G. V. Astakhov, V. Dyakonov, P. G. Baranov, *J. Phys. D Appl. Phys.* **2018**, *51*, 333002.
[112] C. Godfrin, S. Lumetti, H. Biard, E. Bonet, S. Klyatskaya, M. Ruben, A. Candini, M. Affronte, W. Wernsdorfer, F. Balestro, *J. Appl. Phys.* **2019**, *125*, 142801.
[113] R. Wiesendanger, H. J. Gïtherodt, G. Gïtherodt, R. J. Gambino, R. Ruf, *Phys. Rev. Lett.* **1990**, *65*, 247.
[114] R. Wiesendanger, *Rev. Mod. Phys.* **2009**, *81*, 1495.
[115] P. Willke, K. Yang, Y. Bae, A. J. Heinrich, C. P. Lutz, *Nat. Phys.* **2019**, *15*, 1005.
[116] P. Willke, Y. Bae, K. Yang, J. L. Lado, A. Ferrón, T. Choi, A. Ardavan, J. Fernández-Rossier, A. J. Heinrich, C. P. Lutz, *Science* **2018**, *362*, 336.
[117] K. Yang, W. Paul, S. H. Phark, P. Willke, Y. Bae, T. Choi, T. Esat, A. Ardavan, A. J. Heinrich, C. P. Lutz, *Science* **2019**, *366*, 509.
[118] P. Willke, A. Singha, X. Zhang, T. Esat, C. P. Lutz, A. J. Heinrich, T. Choi, *Nano Lett.* **2019**, *19*, 8201.
[119] P. Willke, W. Paul, F. D. Natterer, K. Yang, Y. Bae, T. Choi, J. Fernández-Rossier, A. J. Heinrich, C. P. Lutz, *Sci. Adv.* **2018**, *4*, eaaq1543.
[120] K. Yang, Y. Bae, W. Paul, F. D. Natterer, P. Willke, J. L. Lado, A. Ferrón, T. Choi, J. Fernández-Rossier, A. J. Heinrich, C. P. Lutz, *Phys. Rev. Lett.* **2017**, *119*, 227206.
[121] Y. Bae, K. Yang, P. Willke, T. Choi, A. J. Heinrich, C. P. Lutz, *Sci. Adv.* **2018**, *4*, eaau4159.
[122] P. W. Shor, *SIAM J. Comput.* **1997**, *26*, 1484.
[123] L. K. Grover, *Phys. Rev. Lett.* **1997**, *79*, 325.
[124] F. Troiani, A. Ghirri, M. Affronte, S. Carretta, P. Santini, G. Amoretti, S. Piligkos, G. Timco, R. E. P. Winpenny, *Phys. Rev. Lett.* **2005**, *94*, 207208.
[125] D. Aguilà, L. A. Barrios, V. Velasco, O. Roubeau, A. Repollés, P. J. Alonso, J. Sesé, S. J. Teat, F. Luis, G. Aromí, *J. Am. Chem. Soc.* **2014**, *136*, 14215.
[126] K. S. Pedersen, A. M. Ariciu, S. McAdams, H. Weihe, J. Bendix, F. Tuna, S. Piligkos, *J. Am. Chem. Soc.* **2016**, *138*, 5801.
[127] A. Chiesa, G. F. S. Whitehead, S. Carretta, L. Carthy, G. A. Timco, S. J. Teat, G. Amoretti, E. Pavarini, R. E. P. Winpenny, P. Santini, *Sci. Rep.* **2014**, *4*, 7423.
[128] A. Chiesa, P. Santini, S. Carretta, *Magnetochemistry* **2016**, *2*, 37.
[129] M. Atzori, A. Chiesa, E. Morra, M. Chiesa, L. Sorace, S. Carretta, R. Sessoli, A. Chiesa, M. Chiesa, R. Sessoli, E. Morra, L. Sorace, M. Atzori, A. Chiesa, E. Morra, M. Chiesa, L. Sorace, S. Carretta, R. Sessoli, *Chem. Sci.* **2018**, *9*, 6183.
[130] F. Tacchino, A. Chiesa, R. Sessoli, I. Tavernelli, S. Carretta, *J. Mater. Chem. C Mater.* **2021**, *9*, 10266.
[131] M. D. Jenkins, Y. Duan, B. Diosdado, J. J. García-Ripoll, A. Gaita-Ariño, C. Giménez-Saiz, P. J. Alonso, E. Coronado, F. Luis, *Phys. Rev. B.* **2017**, *95*, 064423.
[132] M. J. Martínez-Pérez, S. Cardona-Serra, C. Schlegel, F. Moro, P. J. Alonso, H. Prima-García, J. M. Clemente-Juan, M. Evangelisti, A. Gaita-Ariño, J. Sesé, J. Van Slageren, E. Coronado, F. Luis, *Phys. Rev. Lett.* **2012**, *108*, 247213.
[133] F. Luis, P. J. Alonso, O. Roubeau, V. Velasco, D. Zueco, D. Aguilà, J. I. Martínez, L. A. Barrios, G. Aromí, *Commun. Chem.* **2020**, *3*, https://doi.org/10.1038/s42004-020-00422-w.
[134] E. M Pineda, T. Komeda, K. Katoh, M. Yamashita, M. Ruben, *Dalton Trans.* **2016**, *45*, 18417.
[135] S. Chicco, G. Allodi, A. Chiesa, E. Garlatti, C. D. Buch, P. Santini, R. De Renzi, S. Piligkos, S. Carretta, *J. Am. Chem. Soc.* **2024**, *146*, 1053.
[136] A. Chiesa, P. Santini, E. Garlatti, F. Luis, S. Carretta, *Rep. Prog. Phys.* **2024**, *87*, 034501.
[137] I. Gimeno, A. Urtizberea, J. Román-Roche, D. Zueco, A. Camón, P. J. Alonso, O. Roubeau, F. Luis, *Chem. Sci.* **2021**, *12*, 5621.
[138] M. Atzori, E. Garlatti, G. Allodi, S. Chicco, A. Chiesa, A. Albino, R. De Renzi, E. Salvadori, M. Chiesa, S. Carretta, L. Sorace, *Inorg. Chem.* **2021**, *60*, 11273.
[139] S. Carretta, D. Zueco, A. Chiesa, F. L. Gómez-León, *Appl. Phys. Lett.* **2021**, *118*, 240501.
[140] Á. Gómez-León, F. Luis, D. Zueco, *Phys. Rev. Appl.* **2022**, *17*, 064030.
[141] A. Castro, A. García Carrizo, S. Roca, D. Zueco, F. Luis, *Phys. Rev. Appl.* **2022**, *17*, 064028.

Eufemio Moreno-Pineda is a scientist specialising in molecular magnetism. He is currently an Alexander von Humboldt fellow at the Physikalisches Institut at Karlsruhe Institute of Technology. He has been recognized for his contributions to science by the Leonard Rieser Young Scientist Award in 2022. His research focuses on the development of molecular magnetic systems for use in quantum technologies, such as qubits and qudits, with the aim of implementing these systems in spintronics, and quantum technologies. Currently, he focuses on the magnetic characterisation of molecular magnets via μSQUID and μSQUID-EPR techniques.

Wolfgang Wernsdorfer is a leading physicist in nanomagnetism and quantum computing, currently a Humboldt Professor at the Karlsruhe Institute of Technology (KIT). He has made pioneering contributions to molecular spintronics and the development of quantum bits using molecular systems. His work on single-molecule magnets has significantly advanced the field of quantum nanomagnetism. Wernsdorfer has published extensively and received numerous awards, including the Gottfried Wilhelm Leibniz Prize in 2019. His research aims to create scalable and efficient quantum computing technologies by exploring the quantum properties of molecular systems.